COMUTATIONAL STUDY OF OXYGEN AND GLUCOSE TRANSPORT IN ENGINEERED CARTILAGE CONSTRUCTS

T.-H. Lin [*] **C.-H. Lin** [*]

Department of Mechanical Engineering
National Central University
Jhongli, Taiwan 32001, R.O.C.

C. A. Chung [**]

Department of Mechanical Engineering
National Central University
Jhongli, Taiwan 32001, R.O.C.

Institute of Biomedical Engineering
National Central University
Jhongli, Taiwan 32001, R.O.C.

ABSTRACT

This paper characterizes the mass transfer and replenishment of glucose and oxygen in tissue engineered cartilage constructs by a numerical approach. Cell population growth modulated by glucose and oxygen is incorporated in the mathematic model. The distribution of synthesized type II collagen and its influence on mediating the chondrocyte growth over scaffold are also investigated. Results from simulation are compared with the experiments in literature to verify the formulation and predictions. It is found that, under static culture, the oftentimes observed phenomenon that the overall cell number densities in thick scaffolds are smaller than in thin scaffolds is mainly due to depletion of glucose rather than oxygen. Cell growth is found to be more sensitive to the change in glucose concentration for thick scaffolds, whereas to be more sensitive to the change in oxygen concentration for thin scaffolds. Results also demonstrate the modulation of chondrocyte growth by type II collagen, presenting the biphasic impact of type II collagen which promotes chondrocyte growth in the initial phase of cultivation, while inhibits cell growth in the long term. The numerical model provides a useful reference for developing cartilaginous constructs in tissue engineering.

Keywords : Cartilage construct, Glucose, Mathematical model, Mass transfer, Oxygen.

1. INTRODUCTION

Every year there are many patients suffering tissue and organ deficiencies. Tissue engineering has been trying to repair, maintain and replace the damaged tissues and organs by developing biological substitutes based on the knowledge of life science and engineering [1,2]. It is hoped that in the future patients who need organ or tissue transplantation may benefit from this emerging medical technology. Since monolayer growth has been demonstrated failing to regenerate three-dimensional tissues, recent advances in tissue engineering have been trying to cultivate cells with porous scaffolds that are devised to accommodate cells, guide cell growth and assemble cells with extracellular matrices (ECMs) into three dimensional tissue implants [3].

Developing three-dimensional cellular scaffolds relies extensively on empirical efforts, demanding many expensive and time-consuming experimental works. Theoretical modeling provides a useful means to help elucidate experimental results and can be employed to optimize the culturing parameters. Most of the tissue engineering mathematical models have been based on the continuum assumption, which treats cells and ECMs as distributed continuums using volume fractions as the variables of space and time. The advantage of using such approaches is that the computational time and storage can be greatly reduced. Freed *et al*. in 1994 formulated an empirical equation for analyzing cell culture on a polyglycolic acid (PGA) scaffold [4,5]. Later, models that measure cell density distribution and oxygen concentration over scaffold were set up [6,7]. More recently, research efforts have been devoted to develop more comprehensive models that treat the cell-scaffold construct as a porous medium using the volume average method in order to elucidate the distribution of nutrients and their effects on cell growth [8-11].

To date, the individual effects of oxygen [7,12,13] and glucose [8-11] on modulating the development of cellular scaffolds have already been demonstrated. The simultaneous uptakes of glucose and oxygen by

[*] Graduate student [**] Professor, corresponding author

DOI : 10.1017/jmech.2011.36
Copyright © 2011 The Society of Theoretical and Applied Mechanics, R.O.C.
https://doi.org/10.1017/jmech.2011.36 Published online by Cambridge University Press

chondrocytes have also been reported [15-17]. However, the simultaneous transport and influence of both nutrients on cell growth have yet been studied. Since the diffusion of oxygen in water is one order greater than that of glucose, the time scales of delivery rate of these two nutrients should be distinct, and may to some extent affect the cell growth that responds to nutrient distribution over scaffold. Moreover, in addition to nutrients, type II collagen, as the major extracellular substrate in cartilage, is believed to be able to regulate the chondrocyte growth too. It was shown experimentally that collagen expresses a biphasic influence on cell proliferation. That is cell growth is promoted by collagen monomers while inhibited by collagen polymers [18-20]. In order to depict the development of cellular scaffolds, complete mathematical models incorporating nutrients as well as ECM modulation on constructing cellular scaffolds cannot be overemphasized. Previously, a mathematical model that involves the glucose and collagen modulations on chondrocyte cultures has been set up [11]. The present paper extends that model, incorporating the simultaneous effects of glucose and oxygen, as well as the biphasic impact of collagen on growing chondrocytes under static culture. Results from simulation are compared with the experimental data in literature [4,5], investigating the transport of nutrients in cartilaginous constructs of different thicknesses, to verify the formulation. The relative significance of glucose and oxygen on mediating chondrocyte growth in scaffolds is then demonstrated. Collagen distribution and its influence on cell growth are presented too.

2. MATHEMATICAL FORMULATION

The schematic of the static culture system considered in this work is shown in Fig. 1, compliant to the experimental sets of Freed *et al*. [4,5] which investigated the cartilaginous constructs with bovine chondrocytes seeded in PGA polymers (above 90% porosity). The inoculated scaffolds immersed in the culture medium were placed in the Petri dish. The medium contains necessary nutrients and growth factors (soluble proteins serving as intercellular chemical messengers) for normal tissue development. The present model focuses on the transport phenomena of glucose and oxygen. Oxygen diffuses from the ambient air across the free surface, through the culture medium, and eventually into the scaffold. Glucose diffuses into the scaffold from the surrounding culture medium, and is restored by replenishing half the culture medium every three days. Cells in scaffolds are considered to proliferate under the influences of oxygen and glucose to populate the construct and form the artificial implants. Collagen secreted by cells also plays a part in modulating cell growth. Cells in the scaffold were assumed to be able to migrate in all directions without any directional preference. In summary, the model includes four mass phases: Oxygen, glucose, cells and collagen. Their spatiotemporal evolutions in the scaffold are depicted by the following formulation.

2.1 Nutrient Balance in Culture Medium

No cells are assumed to reside in the culture medium; accordingly there is no nutrient consumption that occurs in the surrounding medium. The governing equations for oxygen and glucose in the culture medium region thus are of a pure diffusion form, which read [14,15]

$$\frac{\partial C_{\mathrm{f}}^{i}}{\partial t}=\nabla\cdot(D_{\mathrm{f}}^{i}\,\nabla C_{\mathrm{f}}^{i}) \tag{1}$$

where C_{f}^{i} is the nutrient concentration in the culture medium with the superscript i = oxy and i = glu referring to oxygen and glucose respectively. The nutrient diffusion coefficients D_{f}^{i} are assumed to be constants.

2.2 Nutrient Balance in Scaffold

In scaffolds, oxygen and glucose are diffusive through interconnected pores and consumed by cells. These phenomena may be described by the diffusion-reaction equations as follows [14,15]

$$\frac{\partial C_{\mathrm{s}}^{i}}{\partial t}=\nabla\cdot(D_{\mathrm{eff}}^{i}\,\nabla C_{\mathrm{s}}^{i})-N_{\mathrm{c}}\,Q^{i} \tag{2}$$

where C_{s}^{i} is the nutrient concentration in the scaffold with the superscript i = oxy and i = glu denoting oxygen and glucose respectively, D_{eff}^{i} is the effective diffusivity of oxygen and glucose respectively. The effective diffusivities are assumed to be constants for simplicity. As the cells grow, pore size and porosity change. To account for the effects of changing porosity on reducing nutrient diffusion, more sophisticate formulae such as the Mackie and Meares equation can be used [21]. However, on condition that reduction in the construct pores retards both the transport of oxygen and glucose, the relative ratio of the nutrient diffusivities virtually retains the same order of magnitude. Therefore, we assume constant diffusion coefficients so as to focus on studying the relative significance of nutrient transport instead of the porosity change on nutrient deliveries. Furthermore, N_c is the cell number density, and Q^i the nutrient consumption rate for oxygen and glucose respectively. We use the Michaelis-Menten equation to describe Q^i as [8,9,13,22]

$$Q^{i}=\frac{Q_{\max}^{i}\,C_{\mathrm{s}}^{i}}{K_{\mathrm{m}}^{i}+C_{\mathrm{s}}^{i}} \tag{3}$$

where $Q_{\max}^{i}$ is the maximum nutrient uptake rate, and K_{m}^{i} the saturation coefficient which gives $Q^{i}=Q_{\max}^{i}/2$ at $C_{\mathrm{s}}^{i}=K_{\mathrm{m}}^{i}$. Chondrocytes may consume oxygen at different rates depending on the glucose concentration in their surrounding medium. Literature [16] showed experimentally that, when glucose concentrations are higher than 1mM (0.18mg/cm^3), bovine chondrocytes consume oxygen at a relatively constant

https://doi.org/10.1017/jmech.2011.36 Published online by Cambridge University Press

rate; Oxygen consumption rate increases profoundly only when glucose levels drop below 1mM (the Crabtree effect). Since the average glucose concentration over scaffold is considered to be larger than 1mM in this work, the dependence of the nutrient uptake rates has been ignored in the present model.

2.3 Cell Balance in Scaffold

The cell balance equation in scaffolds is derived based on consideration of cell mass conservation, which yields [10]

$$\frac{\partial N_c}{\partial t} = D_c \nabla^2 N_c + \mu_{g,cell} N_c - \mu_{d,cell} N_c \tag{4}$$

where the constant D_c is the coefficient of cell random motility that is used to describe the macroscopic cell population migration due to random walks [10], and $\mu_{d,cell}$ is the cell apoptosis rate which is assumed as a constant [10]. To model the cell growth under the influence of nutrients and type II collagen, the cell growth rate may take the following form [22]

$$\mu_{g,cell} = \mu_{cell}\left(\frac{C_s^{oxy}}{K_c^{oxy}+C_s^{oxy}}\right)\left(\frac{C_s^{glu}}{K_c^{glu}+C_s^{glu}}\right)\left(\frac{C_{col}}{K_{col}^2+C_{col}^2}\right) \tag{5}$$

where μ_{cell} is a constant. The modulations by oxygen and glucose are assumed to take the Monod kinetics with K_c^{oxy} and K_c^{glu} being the corresponding half maximum rate concentrations. The dependence of cell growth on collagen is described by the last term, which is essentially a biphasic function of collagen content, whereby cell growth rate increases and then decreases as collagen increases in amount [11,23]. Previous research evidenced that cell proliferation is promoted by monomeric collagen while inhibited by collagen polymers [18-20,24]. To include these two competing mechanisms, collagen is assumed to be of monomers or polymers depending on the collagen concentration due to the fact that collagen is monomeric when newly secreted by cells and then increase in amount and eventually polymerized into fibrils.

2.4 Collagen Balance in Scaffold

Human cartilages are comprised majorly of water and solid matrix. Water occupies about 75% of the entire volume. The remaining space is filled with extracellular matrix. From the whole volume of the extracellular matrix, collagens occupy 65%, proteoglycans 25%, and glycoproteins, chondrocytes and lipids take the remaining 10% [25]. As for collagens, type II occupies 90-95% v/v [26]. Therefore, type II collagen is taken as the representative ECM component in this work. To formulate the coupling effects between the cell proliferation and the secretion and accumulation of type II collagen, the equation describing secretion and degradation of collagen takes the following form [23]

$$\frac{\partial C_{col}}{\partial t} = N_c(\gamma_{g,col} - \gamma_{d,col} C_{col}) \tag{6}$$

where $\gamma_{g,col}$ and $\gamma_{d,col}$ refer to the collagen secretion and degradation rate respectively.

2.5 Initial and Boundary Conditions

Appropriate initial and boundary conditions are needed for solving the governing equations. Cell culture incubators typically contain 5% CO_2 in the air, which changes the environmental oxygen concentration from 21% to 20%. Based on considering oxygen is dissolved into the medium at the rate of 10.268μM per percentage partial volume of O_2 in air [27], the initial condition of oxygen concentration is set as 200μM, which is equivalent to

$$C_0^{oxy} = 6.4\mu g/cm^3 \tag{7}$$

As for the initial conditions for glucose and cell number density, they are set compliant to the experiments of Freed *et al*. [4], which gives

$$C_0^{glu} = 4.5mg/cm^3 \tag{8}$$

$$N_c = N_0^{eff} \tag{9}$$

where the initial value of cell number density is chosen following the experiments as $N_0^{eff} = 1.319\times10^7$, 0.909×10^7, and 1.192×10^7cells/cm^3 for the scaffold thickness of 0.116, 0.168 and 0.384cm respectively. Collagen is assumed to be null in the initial state, that is

$$C_{col} = 0 \tag{10}$$

Half the culture medium is replenished every three days, which is simulated by resetting the nutrient concentration in the culture medium surrounding the scaffold as

$$C_f^i = (C_0^i + C_{f,avg}^i)/2 \tag{11a}$$

$$\text{with} \quad C_{f,avg}^i = \int_V C_f^i dV/V \tag{11b}$$

being the volume average nutrient concentration in the medium right before replenishment.

As for the boundary conditions, the computational domain is assumed to be axisymmetric along the center line, therefore axisymmetric conditions are used for the nutrient concentration and cell number density at boundary 1 and for the nutrients at boundary 2 (Fig. 1):

$$\nabla C_s^i \cdot \mathbf{n} = 0, \ \nabla N_c \cdot \mathbf{n} = 0 \ \text{ at boundary 1} \tag{12}$$

$$\nabla C_f^i \cdot \mathbf{n} = 0 \quad \text{at boundary 2} \tag{13}$$

https://doi.org/10.1017/jmech.2011.36 Published online by Cambridge University Press

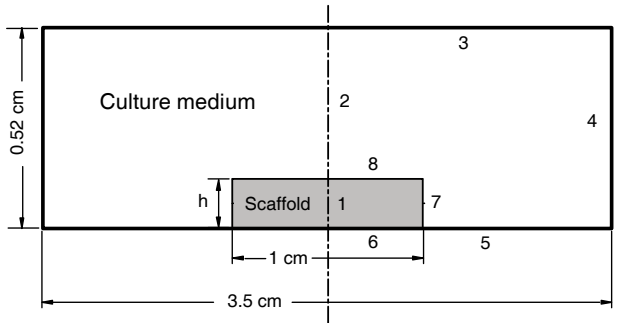


Fig. 1 Schematic diagram of the static culture system (dimensions are not to scale). A cellular construct immersed in the culture medium is placed in the middle of the Petri dish plate. The numbers denote the boundaries of the simulation domain, which is a radial section for simplicity of axisymmetry

where **n** is the unit normal vector at the boundary. The culture medium is open to the air, therefore oxygen is assumed to dissolve into the medium through boundary 3. On the other hand, glucose is added only by medium replacement; it has zero mass flux at the free surface. In summary, the boundary conditions for oxygen and glucose at the free surface are

$$C_{\mathrm{f}}^{\mathrm{oxy}} = C_0^{\mathrm{oxy}}\ ,\ \nabla C_{\mathrm{f}}^{\mathrm{glu}} \cdot \mathbf{n} = 0 \quad \text{at boundary 3} \tag{14}$$

Boundaries 4 and 5 denote the Petri dish wall and bottom plate respectively, therefore there is no nutrient flux across these boundaries, which yields

$$\nabla C_{\mathrm{f}}^{\mathrm{i}} \cdot \mathbf{n} = 0 \quad \text{at boundaries 4, 5} \tag{15}$$

Similarly as the scaffold is placed on the dish plate, no transport of nutrients and cell can occur at the boundary, which yields

$$\nabla C_{\mathrm{s}}^{\mathrm{i}} \cdot \mathbf{n} = 0\ ,\ \nabla N_{\mathrm{c}} \cdot \mathbf{n} = 0 \quad \text{at boundary 6} \tag{16}$$

At the interface of scaffold with the culture medium, we consider nutrient concentrations and fluxes are continuous, and cells cannot move out of the scaffold, which yields

$$\begin{aligned} &C_{\mathrm{s}}^{i} = C_{\mathrm{f}}^{i}\ ,\quad D_{\mathrm{f}}^{i}\nabla C_{\mathrm{f}}^{i} \cdot \mathbf{n} = D_{\mathrm{eff}}^{i}\nabla C_{\mathrm{s}}^{i} \cdot \mathbf{n}\ , \\ &\nabla N_{\mathrm{c}} \cdot \mathbf{n} = 0 \quad \text{at boundaries 7, 8} \end{aligned} \tag{17}$$

The governing equations subject to the initial and boundary conditions are solved for oxygen and glucose concentrations both in the culture medium and scaffold regions. The cell number density and collagen concentration are solved in the scaffold. A finite element code, COMSOL Multiphysics 3.2 (COMSOL, Sweden) was employed to perform the computations. Triangular elements with the second-order Lagrange shape functions were used. Tests for grid independence were performed by refining the mesh size until the relative and absolute changes in observed results are smaller than 10^{-3} and 10^{-4}, respectively. Accordingly the maximum element sizes in the scaffold domain were set as 0.015 times the dimension of scaffold radius, and those in the medium domain were 0.035 times the Petri dish radius. The element size was refined near the interface between the scaffold and culture medium, with maximum sizes 0.01 times associated geometric dimensions. The resulting total number of elements was 4267, 4704 and 6352 for 0.116cm, 0.168cm and 0.384cm-thick scaffold, respectively. Simulations were carried out with three scaffold thicknesses while keeping the same scaffold diameter for fitting the experimental results of Freed *et al*. [4]. Since some parametric values could not be found from the literature, their values were determined by fitting the data of cell number densities and collagen amounts using least squares regression. We employed MATLAB (The MathWorks, Inc., USA) to perform the Nelder-Mead Simplex method for minimizing the squares sum of residuals [28]. Parametric values obtained are listed in Table 1.

3. RESULTS AND DISCUSSION

The average cell number density and collagen content over scaffold for different scaffold thicknesses are shown against cultivation time in Figs. 2(a) and 2(b) respectively. Predictions agree with the experimental data. It is noted that the discrepancy between the experimental and numerical results for h = 0.384cm appears to be more obvious than other two h values. Since the scaffold of h = 0.384cm is much thicker than the other two cases, such a discrepancy suggests that the rates at which collagen are synthesized and degraded may depend on the nutrient and culture environment too, rather than simply constants as have been assumed in the present model. Displayed in Fig. 2(c) is the average value of cell growth rate $\mu_{\mathrm{g,cell}}$ over scaffold (Eq. 5). The average value of each scaffold goes up to a maximum and then declines with time in the long term. The average $\mu_{\mathrm{g,cell}}$ becomes even lower than the cell death rate, $\mu_{\mathrm{d,cell}}$, at about 25 days, resulting in the observed decrease of cell number in the long term as shown in Fig. 2(a). The average $\mu_{\mathrm{g,cell}}$ reaches maximum at about 7 days for the 0.116cm thick scaffold, and at 10 days for the other two scaffolds. These time lengths are close to those in which the collagen concentration C_{col} grows close to the value of K_{col} as indicated in Fig. 2(b). As Eq. 5 reveals, cell growth rates depend on the collagen concentration in the form of $C_{\mathrm{col}}/(K_{\mathrm{col}}^2 + C_{\mathrm{col}}^2)$, which yields a maximum value of $1/2K_{\mathrm{col}}$ at $C_{\mathrm{col}} = K_{\mathrm{col}}$. The predicted cell growth rate declines a little earlier than the time point of $C_{\mathrm{col}} = K_{\mathrm{col}}$. This is because the overall cell growth rate is determined not only by collagen contents but also by glucose and oxygen, which further retard the cell growth due to the diffusion limitations [8-10].

https://doi.org/10.1017/jmech.2011.36 Published online by Cambridge University Press

Table 1 Parametric values

Parameter	Definition	Value	Reference
Substrate parameters			
D_{eff}^{glu}	Glucose diffusivity in scaffold	4.14×10^{-6}cm^2/s	[29]
D_{f}^{glu}	Glucose diffusivity in fluid	9.2×10^{-6}cm^2/s	[30]
D_{eff}^{oxy}	Oxygen diffusivity in scaffold	1.5×10^{-5}cm^2/s	[31]
D_{f}^{oxy}	Oxygen diffusivity in fluid	3×10^{-5}cm^2/s	[32]
$\gamma_{d,col}$	Degradation rate of collagen	1.478×10^{-17}cm^3/cell s	
$\gamma_{g,col}$	Secretion rate of collagen	1.126×10^{-13}mg/cell s	
Metabolic parameters			
K_{m}^{glu}	Saturation constant of glucose uptake	6.3×10^{-2}mg/cm^3	[33]
K_{m}^{oxy}	Saturation constant of oxygen uptake	1.856×10^{-4}mg/cm^3	[34]
Q_{max}^{glu}	Max uptake rate of glucose	3.06×10^{-12}mg/cell s	[35]
Q_{max}^{oxy}	Max uptake rate of oxygen	5.952×10^{-14}mg/cell s	[6]
Cell growth and migration parameters			
D_c	Cell diffusion coefficient	1.7×10^{-10}cm^2/s	[36]
K_{col}	Saturation coefficient to collagen	1.406mg/cm^3	
K_{c}^{glu}	Saturation coefficient to glucose	1.817mg/cm^3	
K_{c}^{oxy}	Saturation coefficient to oxygen	3.068×10^{-2}mg/cell	
$\mu_{d,cell}$	Cell death rate	3.3×10^{-7}1/s	[10]
μ_{cell}	Cell growth rate constant	2.047×10^{-5}mg/cm^3 s (0.116cm thick scaffold) 1.814×10^{-5}mg/cm^3 s (0.168cm thick scaffold) 1.139×10^{-5}mg/cm^3 s (0.384cm thick scaffold)	

The predicted oxygen concentration is displayed in Fig. 3, where the 0.116cm and 0.384cm thick scaffolds at 10 days and 30 days are shown representatively. Consumed by cells, oxygen in the scaffold generally decreases in amount with time. A spatial pattern gradually forms with oxygen becoming most depleted at the central bottom while remaining rich away from the scaffold. This reflects the fact that oxygen is supplied from the ambient air diffusing through the surrounding culture media into the scaffolds. Comparison between the two scaffolds shows that the thicker scaffold contains richer oxygen in the long term. This scenario can be illustrated more clearly by showing the average oxygen concentration over culture medium (Fig. 4(a)) and scaffold (Fig. 4(b)), respectively. For both scaffolds, oxygen concentration goes down abruptly at the beginning of cultivation, and oxygen is consumed more quickly in the 0.384cm case as totally more cells have been seeded in that scaffold. The oxygen concentration becomes lower in the thinner scaffold than in

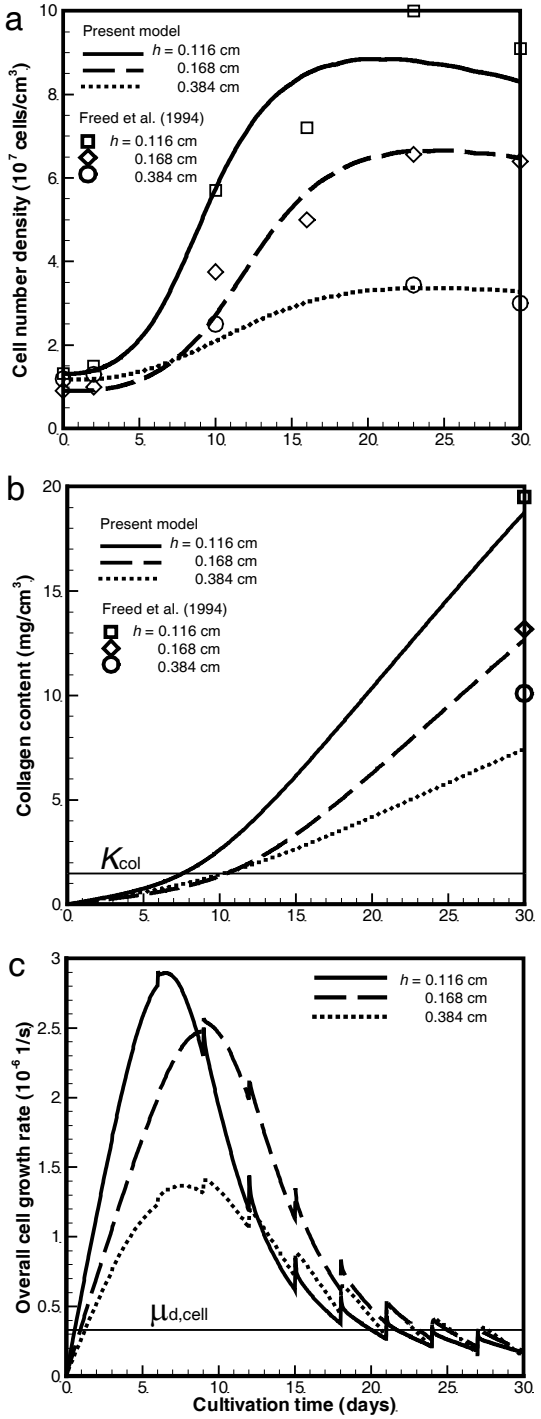


Fig. 2 Comparison of the predicted (a) Average cell number densities and (b) Synthesized collagen concentrations with the experimental data of Freed *et al.* [4] for scaffolds of variant thicknesses. (c) Predictions of average cell growth rate for variant scaffold thicknesses

the thicker scaffold after about 8 days. This is because the thinner scaffold is further away from the free surface of the medium so that oxygen needs to take longer time to reach the scaffold from the ambient air. Note that oxygen concentrations go up and down abruptly every three days reflecting the fact that the culture medium is regularly replenished. The enlarged inset in Fig. 4(b) shows that the abrupt changes in oxygen

https://doi.org/10.1017/jmech.2011.36 Published online by Cambridge University Press

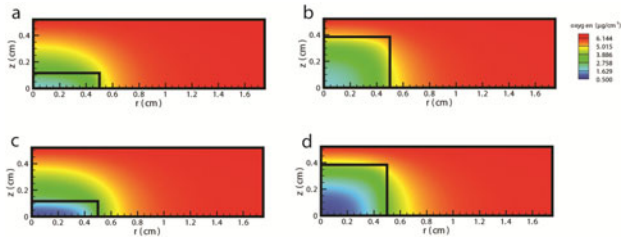
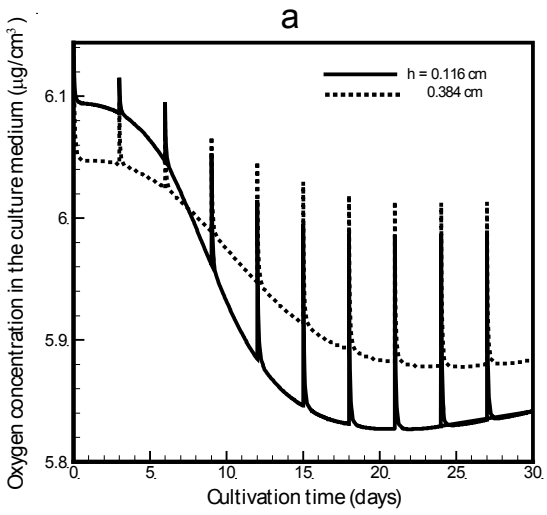


Fig. 3 Contours of oxygen concentration at 10 days of cultivation (top panel) and 30 days of cultivation (bottom panel) for the 0.116cm thick scaffold (a,c) and 0.384cm thick scaffold (b,d) respectively



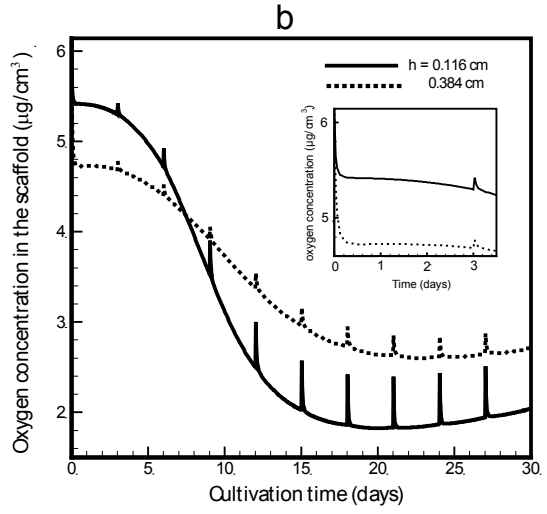


Fig. 4 Temporal evolution of the average oxygen concentration over (a) Culture medium and (b) Scaffold for two scaffolds of different thicknesses. The inset in (b) is the enlargement of oxygen concentration in the scaffold for the time period ranging from $t = 0$ to $t = 3.4$ days

concentration span about 0.2 days (4.8hr). This time period is equivalent to the diffusion time required for oxygen to transfer from the free surface to scaffold. After this period of time, oxygen gets supplied from the free surface; therefore its descending rate slows down. It is also noted that after 20 days of cultivation, the oxygen level becomes even increased with time because the cell number has turned to decrease.

Figure 5 shows the distributions of glucose concentration in the 0.116cm and 0.384cm thick scaffolds at 10 days and 30 days, respectively. Consumed by cells, glucose in the two scaffolds gradually declines in concentration over time. However, it is different from the oxygen case in which oxygen can be continuously supplied from the ambient air. Glucose is added only when the culture medium is replenished. Therefore glucose is relatively depleted under static culture. The thicker the scaffold, the lesser amount of culture medium can be added due to a relative lack of available volume. Accordingly, glucose concentration in the thicker scaffold remains to be lower over time than that in the thinner one. The average glucose concentration over culture medium and scaffold is displayed in Figs. 6(a) and 6(b), respectively. The medium replacement results in glucose concentration rising sharply. Glucose consumption exhibits a nearly constant, sharp decreasing in amount, which is apparently distinct from that of oxygen. Oxygen concentration presents also sharp declination only right after medium is changed. However, as long as oxygen supplied from the ambient air reaches the scaffolds, oxygen contents become to decline moderately. Such is not the case with glucose because glucose gets replenished only when medium is changed every three days.

Cell distribution over scaffold at 30 days is shown in Fig. 7 for the 0.116cm and 0.384cm thick scaffold, respectively. It is apparently noted that the cell number density over the thinner scaffold is larger than that in the thicker one. Such a scenario has been observed experimentally and theoretically in previous literature [4,5,8-13], attributed to the diffusion limit of nutrients. Present work further shows that glucose dominates the limitation over oxygen because, as Fig. 4 reveals, the overall oxygen concentration is smaller in the thinner scaffold than in the thicker one. On the contrary, glucose is shown to be more depleted in the thicker scaffold. Therefore, it is not oxygen but glucose that results in lower cell number densities in thicker scaffolds under static culture. The present study further shows that although glucose determines the final cell number density, oxygen determines the spatial pattern of cell distribution. Such a scenario can be clearly seen especially in the thin scaffolds by comparing Figs. 3 and 7. Collagen is secreted by cells; therefore its distribution and amount generally follow the cell distribution. As Fig. 8 illustrates, the 0.116cm thick scaffold has more collagen concentration than that of the 0.384cm scaffold. Collagen is found to be more concentrated around the scaffold boundary, following the fact that cells are more concentrated around the boundary too.

From the above results, the conclusion on the relative significance of oxygen and glucose on the cell growth in static culture is drawn. The sensitiveness of average cell number density over scaffold to changes in original oxygen and glucose concentrations (±25% of typical values) are evaluated at 30 days for the 0.116cm and 0.384cm thick scaffolds in Figs. 9(a) and 9(b), respectively. It is interesting to note that the predicted

https://doi.org/10.1017/jmech.2011.36 Published online by Cambridge University Press

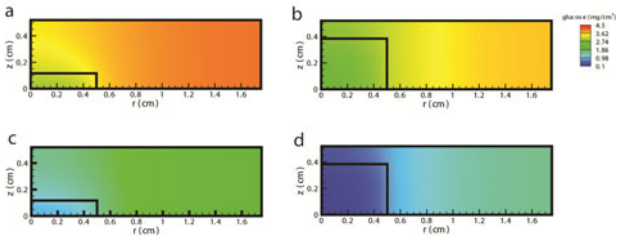


Fig. 5 Contours of glucose concentration at 10 days of cultivation (top panel) and 30 days of cultivation (bottom panel) for the 0.116cm thick scaffold (a,c) and 0.384cm thick scaffold (b,d) respectively

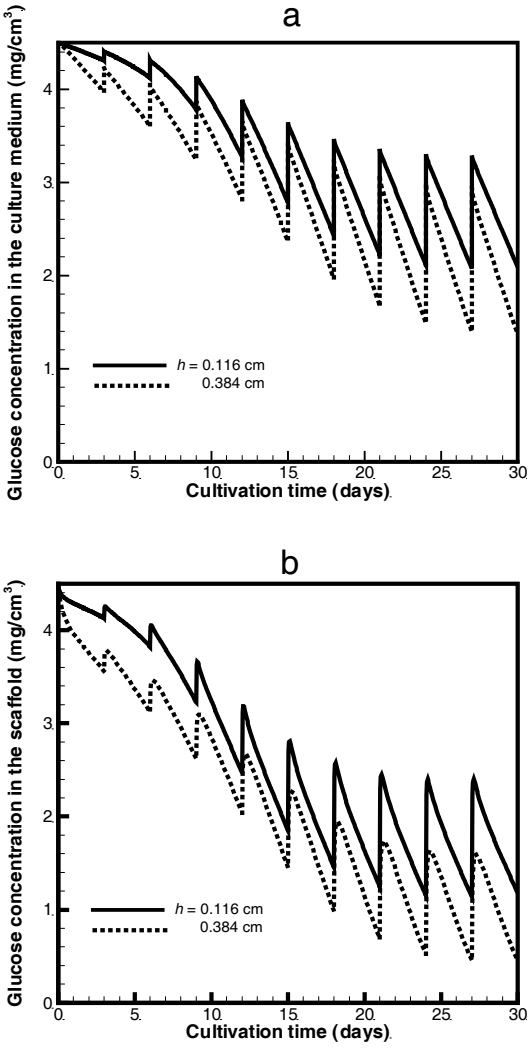


Fig. 6 Temporal evolution of the average glucose concentration over (a) Culture medium and (b) Scaffold for two scaffolds of different thicknesses

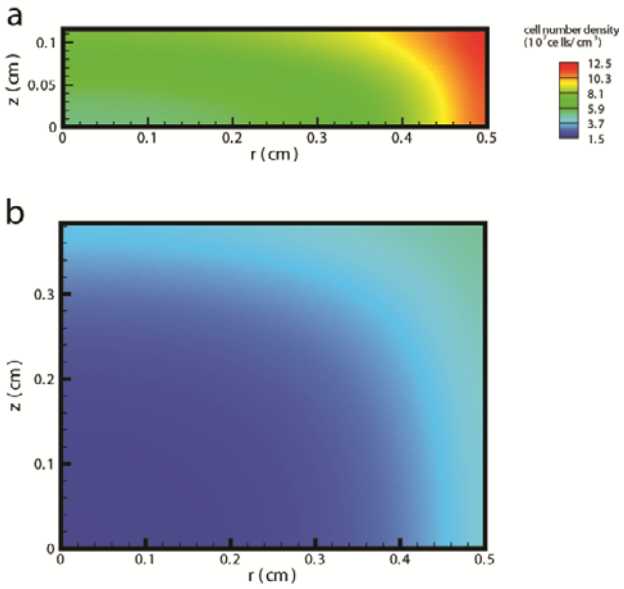


Fig. 7 Contours of cell number density at 30 days of cultivation in (a) The 0.116cm thick scaffold, and (b) The 0.384cm thick scaffold

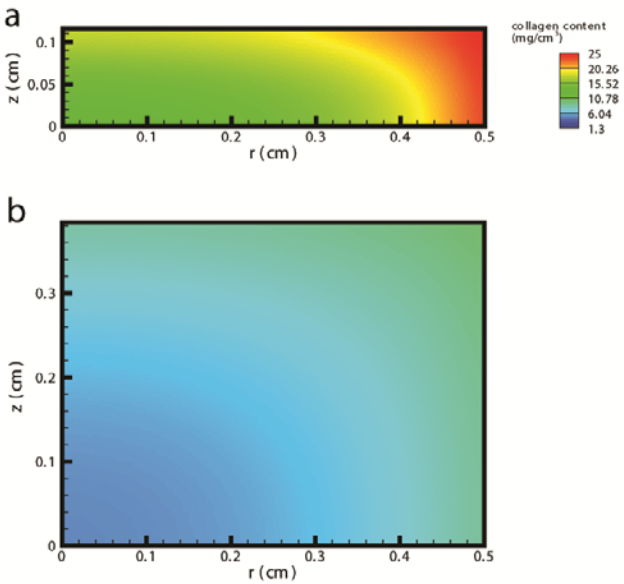


Fig. 8 Contours of collagen concentration at 30 days of cultivation in (a) The 0.116cm thick scaffold, and (b) The 0.384cm thick scaffold

cell number density for thin scaffolds is more sensitive to the change in oxygen concentration than that in glucose. For the thick scaffold, an opposite trend is observed. The reason is that oxygen goes a long diffusion route from the free surface to a thin scaffold; therefore oxygen is relatively depleted in thin scaffolds. On the other hand, for a thick scaffold, the culture medium is less and so the available glucose is relatively depleted. Therefore cell growth in the thicker scaffolds is more sensitive to the increase or decrease in glucose concentration. In summary, cell growth rate is more sensitive to the change of the relatively depleted nutrient.

4. CONCLUDING REMARKS

This paper has performed a numerical study on describing cell growth and collagen accumulation within scaffolds under the modulation by glucose and oxygen. The predictions of chondrocyte proliferation and collagen levels were validated by the experimental data in

https://doi.org/10.1017/jmech.2011.36 Published online by Cambridge University Press

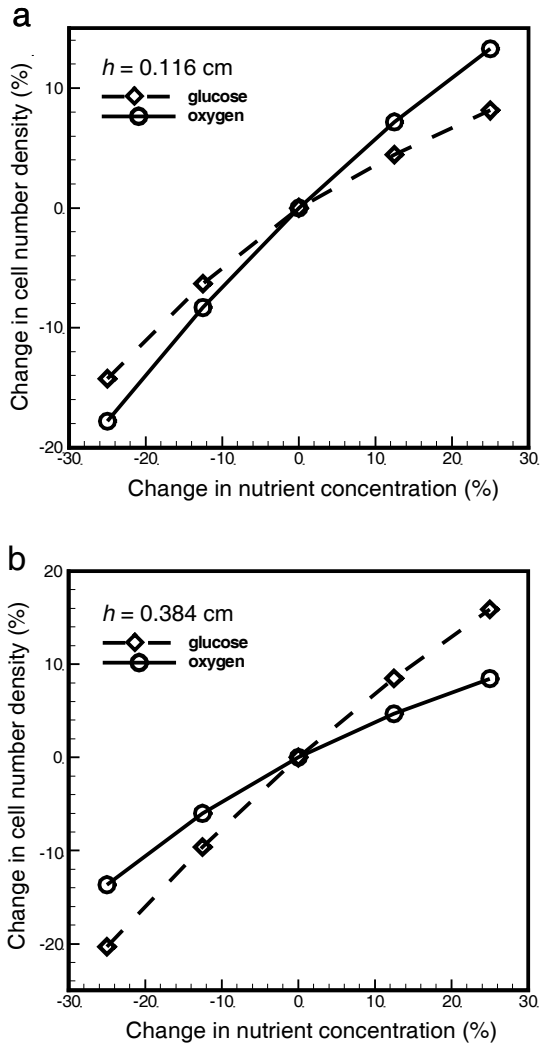


Fig. 9 Sensitivities of average cell number density over scaffold to changes of nutrient concentrations (±25% of typical values) is evaluated at 30 days of cultivation for (a) The 0.116cm thick scaffold, and (b) The 0.384cm thick scaffold

the literature, investigating the development of cartilaginous constructs with various scaffold thicknesses under static cultivation. The model simulated the culture condition in which half the culture medium is replenished every three days. Results from simulation show that the cell number density overall is dominated by glucose level. However, cell growth is more sensitive to glucose or oxygen change depending on which nutrient is relatively depleted over scaffold. The model also incorporates the modulation of chondrocyte growth by type II collagen to account for the biphasic impact that type II collagen put, which promotes chondrocyte growth in the initial phase of cultivation, while inhibits cell growth in the long term. As the contents of glucose eventually determine the overall cell amounts in cartilage constructs especially when cellular scaffolds are getting thicker, designing novel culture systems with the aid of flow dynamics may help deliver efficient glucose to cells for developing cartilage implants of practically large size.

This work considers the combined oxygen and glucose modulation on chondrocyte growth by a double Monod kinetics. The consumption rates of oxygen and glucose are assumed to be independent. Further improvements on the modeling may be made in the future. For example, it was observed that chondrocytes may adjust their metabolic pathway to adapt to the extracellular nutrient environment. Lactate was shown to be produced accompanying the consumption of glucose and the medium would become more acid. Under such a condition, cells may slow down their metabolism to adapt to the environmental change [16]. The current model neglects these coupling effects. It is worthwhile to develop a sophisticated model to account for the coupled metabolic pathways so that more culture conditions can be covered. To this end, incorporating energy metabolism of glycolysis and tricarboxylic acid cycle into the formulation may be helpful to advance the modeling.

In addition to studying the limitation of nutrients, this work also includes the regulation of type II collagen on chondrocyte growth in vitro, using a phenomenological approach. Cell growth is considered to be enhanced by collagen when the collagen amount is small but to be suppressed when the collagen amount is large. The considered mechanism underlying this biphasic scenario is that chondrocyte proliferation is promoted by collagen monomers but inhibited by collagen fibrils [18-20]. As newly synthesized collagen is monomeric and less in quantity, collagen in the initial phase of cell cultivation is modeled to play a promoting role in cell growth. On the other hand, once collagen accumulates and polymerizes into fibrils, it gradually change its role to slow down the cell proliferation in the long term. This work treats the two types of collagen as a whole mass. The individual effect of monomeric and fibrous collagen is worth investigation in the future.

ACKNOWLEDGMENTS

This work is supported by research grants from the National Science Council of Taiwan (NSC 96-2221-E-008-066-MY3) and from the GCH-NCU Joint Research Foundation between the National Central University and Cathay Pacific General Hospital of Taiwan (96GCH-NCU-A2).

REFERENCES

1. Langer, R. and Vacanti, P., "Tissue Engineering," *Science*, **260**, pp. 920–925 (1993).
2. Griffith, L. G. and Naughton, G., "Tissue Engineering – Current Challenges and Expanding Opportunities," *Science*, **295**, pp. 1009–1014 (2002).
3. Pachence, J. M. and Kohn, J., "Biodegradable Polymers," Principles of Tissue Engineering, Lanza, R. P., Langer, R. and Vacanti, J., Eds., Academic Press, pp. 263–277 (2000).

https://doi.org/10.1017/jmech.2011.36 Published online by Cambridge University Press

4. Freed, L. E., Vunjak-Novakovic, G., Marquis, J. C. and Langer, R., "Kinetics of Chondrocyte Growth in Cell-Polymer Implants," *Biotechnology and Bioengineering*, **43**, pp. 597–604 (1994).
5. Freed, L. E., Marquis, J. C., Vunjak-Novakovic, G., Emmanual, J. and Langer, R., "Composition of Cell-Polmer Cartilage Implants," *Biotechnology and Bioengineering*, **43**, pp. 605–614 (1994).
6. Obradovic, B., Meldon, J. H., Freed, L. E. and Vunjak-Novakovic, G., "Glycosaminoglycan Deposition in Eengineered Cartilage: Experiments and Mathematical Model," *AIChE Journal*, **46**, pp. 1860–1871 (2000).
7. Lewis, M. C., MacArthur, B. D., Malda, J., Pettet, G. and Please, C. P., "Heterogeneous Proliferation within Eengineered Cartilaginous Tissue: The Role of Oxygen Tension," *Biotechnology and Bioengineering*, **91**, pp. 607–615 (2005).
8. Galban, C. J. and Locke, B. R., "Effects of Spatial Variation of Cells and Nutrient and Product Concentrations Coupled with Product Inhibition on Cell Growth in a Polymer Scaffold," *Biotechnology and Bioengineering*, **64**, pp. 633–643 (1999).
9. Galban, C. J. and Locke, B. R., "Analysis of Cell Growth Kinetics and Substrate Diffusion in a Polymer Scaffold," *Biotechnology and Bioengineering*, **65**, pp. 121–132 (1999).
10. Chung, C. A., Yang, C. W. and Chen, C. W., "Analysis of Cell Growth and Diffusion in a Scaffold for Cartilage Tissue Engineering," *Biotechnology and Bioengineering*, **94**, pp. 1138–1146 (2006).
11. Chung, C. A. and Ho, S. Y., "Analysis of Collagen and Glucose Modulated Cell Growth within Tissue Engineered Scaffolds," *Annals of Biomedical Engineering,* **38**, pp. 655–1663 (2010).
12. Croll, T. I., Gentz, S., Mueller, K., Davision, M., O'Connor, A. J., Stevens, G. W. and Cooper-White, J. J., "Modelling Oxygen Diffusion and Cell Growth in a Porous, Vascularising Scaffold for Soft Tissue Engineering Applications," *Chemical Engineering Science*, **60**, pp. 4924–4934 (2005).
13. Malda, J. Rouwkema, J. Martens, D. E., le Comte, E. P., Kooy, F. K., Tramper, J., van Blitterswijk, C. A. and Riesle, J., "Oxygen Gradients in Tissue-Engineered PEGT/PBT Cartilaginous Constructs: Measurement and Modeling," *Biotechnology and Bioengineering*, **86**, pp. 9–18 (2004).
14. Zhao, F., Pathi, P., Grayson, W., Xing, Q., Locke, B. R. and Ma, T., "Effects of Oxygen Transport on 3D Human Mesenchymal Stem Cell Metabolic Activity in Perfusion and Static Cultures: Experiments and Mathematical Model," *Biotechnology Progress,* **21**, pp. 1269–1280 (2005).
15. Sengers, B. G., Heywood, H. K., Lee, D. A., Oomens, C. W. J. and Bader, D. L., "Nutrient Utilization by Bovine Articular Chondrocytes: A Combined Experimental and Theoretical Approach," *Journal of Biomechanical Engineering,* **127**, pp. 758–766 (2005).
16. Zhou, S., Cui, Z. and Urban, J. P. G., "Nutrient Gradients in Engineered Cartilage: Metabolic Kinetics Measurement and Mass Transfer Modeling," *Biotechnology and Bioengineering*, **101**, pp. 408–421 (2008).
17. Devarapalli, M., Lawence, B. J. and Madihally, S. V., "Modeling Nutrient Consumptions in Large Flow-Through Bioreactors for Tissue Engineering," *Biotechnology and Bioengineering*, **103**, pp. 1003–1015 (2009).
18. Yoshizato, K., Taira, T. and Yamamoto, N., "Growth Inhibition of Human Fibroblasts by Reconstituted Collagen Fibrils," *Biomedical Research,* **6**, pp. 61–71 (1985).
19. Weinberg, C. B. and Bell, E., "Regulation of Proliferation of Bovine Aortic Endothelial Cells, Smooth Muscle Cells, and Adventitial Fibroblasts in Collagen Lattices," *Journal of Cellular Physiology*, **122**, pp. 410–414 (1985).
20. Koyama, H., Raines, E. W., Bornfeldt, K. E., Roberts, J. M. and Ross, R., "Fibrillar Collagen Inhibits Arterial Smooth Muscle Proliferation through Regulation of Cdk2 Inhibitors," *Cell*, **87**, pp. 1069–1078 (1996).
21. Mackie, J. S. and Meares, P., "The Diffusion of Electrolytes in a Cation-Exchange Resin Membrane I: Theoretical," *Proceedings of the Royal Society of London,* **A232**, pp. 498–509 (1955).
22. Bailey, J. E. and Ollis, D. F., Biochemical Engineering Fundamentals, 2th Eds., McGraw-Hill, p. 392, New-York (1986).
23. Olsen, L., Sherratt, J. A., Maini, P. K. and Arnold, F., "A Mathematical Model for the Capillary Endothelial Cell-Extracellular Matrix Interactions in Wound-Healing Angiogenesis," *IMA Journal of Mathematical Applied Medicinal Biological*, **14**, pp. 261–281 (1997).
24. Tsai, W. B. and Wang, M. C., "Effects of an Avidin-Biotin Binding System on Chondrocyte Adhesion and Growth on Biodegradable Polymers," *Macromolecular Bioscience*, **5**, pp. 214–221 (2005).
25. Khalsa, P. S. and Eisenberg, S. R., "Compressive Behavior of Articular Cartilage is not Completely Explained by Proteoglycan Osmotic Pressure," *Journal of Biomechanics,* **30**, pp. 589–594 (1997).
26. Buckwalter, J. A. and Mankin, H. J., "Articular Cartilage. Part I: Tissue Design and Chondrocyte—Matrix Interactions," *Journal of Bone and Joint Surgery, American Volume,* **79**, pp. 600–611 (1997).
27. Ishihara, H. and Urban, J. P. G., "Effects of Low Oxygen Concentrations and Metabolic Inhibitors on Proteoglycan and Protein Synthesis Rates in the Intervertebral Disc," *Journal of Orthopaedic Research*, **17**, pp. 829–835 (1999).
28. Lagarias, J. C., Reeds, J. A., Wright, M. H. and Wright, P. E., "Convergence Properties of the Nelder-Mead Simplex Method in Low Dimensions," *SIAM Journal on Optimization*, **9**, pp. 112–147 (1998).
29. Allhands, R. V., Torzilli, P. A., Kallfelz, F. A., "Measurement of Diffusion of Uncharged Molecules

https://doi.org/10.1017/jmech.2011.36 Published online by Cambridge University Press

in Articular Cartilage," *The Coruell Veterinsriau*, **74**, pp. 111–123 (1983).
30. Torzilli, P. A., Askari, E. and Jenkins, J. T., "Water Content and Solute Diffusion Properties in Articular Cartilage," Biomechanics of Diarthrodial Joints, Mow, V. C., Ratcliffe, A. and Woo, S.L.-Y., Eds, Springer, pp. 363–390, New-York (1990).
31. Chow, D. C., Wenning, L. A., Miller, W. M. and Papoutsakis, E. T., "Modeling pO2 Distributions in the Bone Marrow Hematopoietic Compartment II: Modified Krogh's Models," *Biophysical Journal,* **81**, pp. 685–696 (2001).
32. Himmelblau, D. M., "Diffusion of Dissolved Gases in Liquids," *Chemical Reviews*, **64**, pp. 527–550 (1964).
33. Windhaber, R. A. J., Wilkins, R. J. and Meredith, D., "Functional Characterisation of Glucose Transport in Bovine Articular Chondrocytes," *Pfluegers Archives*, **446**, pp. 572–577 (2003).
34. Haselgrove, J. C., Shapiro, I. M. and Silverton, S. F., "Computer Modeling of the Oxygen Supply and Demand of Cells of the Avian Growth Cartilage," *American Journal of Physidogy-Cell Physiology,* **265**, pp. C497–C506 (1993).
35. Obradovic, B., Carrier, R. L., Vunjak-Novakovic, G. and Freed, L. E., "Gas Exchange is Essential for Bioreactor Cultivation of Tissue Engineered Cartilage," *Biotechnology and Bioengineering*, **63**, pp. 197–205 (1999).
36. Dickinson, R. B., McCarthy, J. B. and Tranquillo, R. T., "Quantitative Characterization of Cell Invasion in vitro: Formulation and Validation of a Mathematical Model of the Collagen Gel Invasion Assay," *Annals of Biomedical Engineering,* **21**, pp. 679–697 (1993).

(Manuscript received June 29, 2010,
accepted for publication August 30, 2010.)

https://doi.org/10.1017/jmech.2011.36 Published online by Cambridge University Press